ERIM

INFRARED AND OPTICS DIVISION

E83-10348

CR-172673

Report No. 164000-2-T

Second
Type II Quarterly Status and Technical Progress Report
21 December 1982 - 20 March 1983

on

Study on Spectral/Radiometric Characteristics of the Thematic Mapper for Land Use Applications

under

Contract NAS5-27346

with

NASA Goddard Space Flight Center
Greenbelt Road
Greenbelt, Maryland 20771

Submitted by

Environmental Research Institute of Michigan
P.O. Box 8618
Ann Arbor, Michigan 48107

Prepared by: Michael D. Metzler
Co-Investigator

for: William A. Malila
Principal Investigator

Approved by: Robert Horvath
Manager, Information
Processing Department

23 March 1983

Second Quarterly Report

STUDY ON SPECTRAL/RADIOMETRIC CHARACTERISTICS OF THE THEMATIC MAPPER FOR LAND USE APPLICATIONS

1. Objective

The objective of this investigation is to quantify the performance of the TM as manifested by the quality of its image data in order to suggest improvements in data production and to assess the effects of the data quality on its utility for land resources applications. Three categories of this analysis are: a) radiometric effects, b) spatial effects, and c) geometric effects, with emphasis on radiometric effects.

2. Tasks

Four tasks have been established to address the above objective. The first three are to study radiometric performance, spatial performance, and geometric performance, respectively, while the fourth is to study spectral characteristics. In keeping with the identified objective, the radiometric performance study is the major task.

3. Status and Technical Progress

Radiometrically and geometrically corrected Thematic Mapper digital data (CCT-PT) and image products were received for two scenes during this quarter; Scene 40145-14492 (8 Dec Cape Cod), and Scene 40122-16234 (15 Nov Oklahoma). The radiometrically, but not geometrically, corrected data (CCT-AT) have been ordered but not yet received. Raw data (CCT-BT) for these two scenes have not been released as of this time.

William Malila and Michael Metzler presented preliminary findings at the Second Landsat-4 Investigators' Workshop 11-12 January 1983. They also attended the Landsat-4 Scientific Characterization of Early Results Symposium, where the paper "Scan-Angle and Detector Effects in Thematic Mapper Radiometry" by Metzler and Malila was presented. The paper describes the analysis and findings of this investigation to date; it is included in this report as Appendix A.

A paper entitled "The Enhanced Earth Observation Potential Realized With the Thematic Mapper" was presented at the Landsat-4 Session of the 1983 ACSM-ASP Annual Meeting on 17 March 1983.

3.1 Problems

No significant problems were encountered this quarter.

3.2 Accomplishments

The accomplishments to date are described in detail in Appendix A. The findings of this reporting period are summarized here.

3.3 Significant Results

Scan-Direction and Scan-Angle Effects

The observations made during the previous quarter of the change in mean signal level as a function of both scan-angle and scan-direction were studied further. The overall scan-angle effect was found to correspond to that expected based on atmospheric modeling and scene characteristics. An initial, empirical correction model employing exponential decay was developed for the reflective bands in the two scenes analyzed (40049-16262 and 40037-16031). Band 6 was observed to have a significant scan-direction effect which was markedly different than that found in the reflective bands.

Later-Detector Calibration

A low frequency (period of several scan cycles) noise was discovered. This noise was most pronounced in Band 1, Detectors 4, 12, 10, and 8, having amplitudes of approximately 2.0, 1.5, 1.0, and 0.75 quantizing levels, respectively. This low frequency variation in mean signal amplitude was highly correlated among those four Band 1 detectors. Low frequency noise was also observed in Band 7, Detector 7; Band 2, Detector 1; Band 3, Detectors 1 and 16; and Band 5, Detector 10. For the non-Band 1 detectors, the amplitude of the noise is $\lesssim 0.5$ quantizing levels. This noise may be a result of interaction of the DC-restore process with coherent (high frequency) noise found in the system.

3.4 Publications

None

3.5 Recommendations

It is recommended that investigations into the scan-direction effect and low-frequency noise be pursued. Any corrections resulting from such an investigation should be incorporated into a single radiometric correction to minimize quantization and round-off effects.

3.6 Funds Expended

3.7 Data Utility

Thematic Mapper has been shown to provide greater spatial and spectral resolution than the MSS. Correction of the small but significant effects described in this report will be helpful in many applications of the data, essential in some. For studies of waterbodies in particular, where small signal changes can be significant and where Band 1 is very important, the low frequency noise and scan direction effects observed in Band 1 will reduce the utility of the data if they remain uncorrected.

DISTRIBUTION LIST

NASA Goddard Space Flight Center
Greenbelt Road
Greenbelt, Maryland 20771

	Copies
Contracting Officer, Code 284.4	1
Publication Branch, Code 253.1	1
Patent Counsel, Code 204	1
Technical Officer, Mr. Harold Oseroff, Code 902	10

APPENDIX A

SCAN ANGLE AND DETECTOR EFFECTS IN THEMATIC MAPPER RADIOMETRY

Michael D. Metzler
William A. Malila
Environmental Research Institute of Michigan
Ann Arbor, Michigan 48107

SCAN ANGLE AND DETECTOR EFFECTS IN THEMATIC MAPPER RADIOMETRY

Abstract

The effects on Thematic Mapper (TM) radiometry of scan angle and inter-detector differences were analyzed. Radiometric corrections currently performed were found to improve overall consistency of data, but some residual striping remains in the corrected data due to the quantization of signal values and other effects. A new type of banding was discovered which is related to the bidirectional scanning of TM. An initial empirical model was developed for correcting this effect in Band 1, but should receive additional development. The scan angle effects observed corresponded to those expected based on atmospheric considerations and scene characteristics. Low frequency scan-to-scan noise was detected in Band 1, Band 7 and to a lesser extent in Bands 2 and 3. The Band 1 detectors which exhibited this noise showed strong correlation in their variation.

INTRODUCTION

This investigation was directed at quantifying and understanding the scan-angle and detector effects observed in TM radiometry.

DATA AND METHODS OF ANALYSIS

The data set used for this study consisted of computer compatible tapes (CCT's) of raw data (CCT-BT), radiometrically corrected data (CCT-AT), and geometrically corrected data (CCT-PT) for two scenes, 40049-16262 (North Central Iowa) and 40037-16031 (Arkansas). Major emphasis was given to the unresampled (CCT-BT and CCT-AT) data to allow analysis of individual scan and detector effects. Although analysis was concentrated on the Iowa scene because of its cloud-free, relatively homogeneous scene content, all analyses were performed for both scenes for

confirmation of results. The analyses were performed over the full frame of data for each band, for each detector within each band and for each scan direction.

Histograms of the frequency of occurrence of each quantized signal level were produced and analyzed for each step in the correction process (CCT-BT to CCT-AT to CCT-PT). Signal means and variances were computed, again before and after calibration. Across track profiles of the mean signal as a function of pixel number were generated for each scan direction by dividing the scene into forward and reverse scans and then computing the mean signal for each set of scans in a window 16 samples wide by 2992 lines (i.e., all forward or all reverse lines) long. Stepping the window across the scene produced relatively noise-free average scan lines exhibiting only gross scene content effects. Along track profiles were generated for each detector by computing the mean signal level for all the pixels in each scan line and then plotting the scan-line means for a given detector as a function of scan number (374 scans x 16 detectors = 5984 lines in full scene, CCT-BT or CCT-AT).

RESULTS

The overall quality of TM imagery was observed to be good. However, several effects were noted which could be significant in analysis of data from different scenes, from different areas within the same scene or for applications where small signal differences are important.

Scan Angle and Scan Direction Effects

Scan angle effects caused by atmospheric backscattering, changing optical path lengths, and ground bidirectional reflectance effects were expected. Figure 1 illustrates the mean signal level as a function of scan angle (pixel number) for each of the seven TM bands. The sharp peaks present are primarily due to urban areas (at pixels 800, 3300), larger bodies of water (pixels 4200-5200), or numerous smaller bodies of water. The feature of interest, however, is the overall decline in mean signal level in going from the western side of the scene to the eastern side. The effect is greatest in Bands 1 and 2 which decrease approximately 10%. Band 3 exhibits a somewhat less apparent angular effect, and the remaining reflective bands demonstrate an even lesser effect and more influence of scene composition. The thermal band, Band 6, also exhibits a similar pattern, with larger responses at the western edge, presumably due to viewing a greater percentage of sunlit scene components. However, this full-frame average scan line for the thermal band masks a distinctive scan-direction effect which is discussed in detail later.

Previous modeling work at ERIM for analyses of spaceborne scanner data have predicted atmospheric scan angle effects similar to those seen with this TM data [1,2]. Figure 2 is a plot of model results derived by us from the data set of Dave [3] for the MSS; their approximate TM equivalents are given. At the longer wavelengths, e.g., TM Bands 4, 5 and 7, atmospheric scan angle effects are reduced, and canopy shadowing and

bidirectional reflectance effects become the predominant drivers of the observed scan-angle effect.

Quantification of the scan-angle effects in TM radiometry was complicated by a new effect which was discovered. Figure 3 illustrates the mean signal level as a function of scan angle for Bands 1 and 6 as in Figure 1, but in Figure 3 the forward and reverse scans are plotted separately. While the dominant effect is the expected scan angle effect, a systematic droop of signal values during the active scan tends to increase the observed scan angle effect for forward scans, and decrease it during reverse scans. This scan direction effect was detected to some extent for all of the reflective bands, and was most pronounced in Band 1. Band 6 also demonstrated a pronounced scan direction effect, but of a distinctly different nature (see Figure 3).

In order to characterize the scan direction effect, the ratio of forward scan signal level to reverse scan signal level was computed as a function of scan angle (pixel). These data (Figure 4) were then fit to an exponential decay model of the form

$$S(p) = \frac{S_0(p)}{1 + A[\exp(-KM) - 1]}$$

where

p = Pixel number, counting from West edge of scene

p_f, p_r = Pixel offsets to convert "p" to relative minor frame number

M = $p_f + p$ for forward scans
$p_r - p$ for reverse scans

$S_0(p)$ = Signal returned to sensor for pixel "p"

$S(p)$ = Corrected signal value for pixel "p"

K = Time constant (reciprocal of the number of pixels of active scan required for 63% of the decay to occur)

A = Factor determining magnitude of total decay

The model was fit with the constraint that A and K be identical for forward and reverse scans. The result of fitting this model to Band 1 of the Iowa scene is illustrated in Figure 4, and in Figure 5 the predicted signal decay during forward and reverse scans is shown. From this model, one can see that the decay begins prior to the first pixel, having decayed approximately 1% by that time. The total decay is approximately 2.25% by the end of the active scan. This results in the mean signal level of the forward scan being approximately 0.75 counts higher than the mean signal level of the reverse scan at the West end of the scene, and approximately 0.75 counts lower at the East end of the scene for Band 1.

For this case (Band 1, scene 40049-16262) the p_f and p_r required for the fit resulted in the exponential decay beginning at the time of DC restore (different times for the two scan directions). During DC restore, a dark (no radiance) level is presented to the detectors, and a DC level capacitor is charged to a value which results in approximately two signal counts. This charge is to be held for the entire scan, having a time constant on the order of minutes [4]. The empirically derived scan-direction effect model suggests that this charge may be decaying much faster (time constant of the order of 10 msec). Two problems exist with this explanation: 1) 10 msec is much, much less than minutes and 2) the magnitude of the effect appears to be proportional to the mean signal level, while the DC restore capacitor simply adds a set signal level. Final explanation of the effect awaits further investigation.

Any corrections for this scan-direction effect should be made an integral part of a single radiometric correction process to minimize quantization and roundoff errors.

Inter-Detector Calibration Effects

Horizontal striping is commonly found in imagery from sensors that scan arrays of detectors. To minimize the potential for striping among the 16 detectors in each band (four in Band 6), a histogram normalization technique is included in the radiometric correction processing. This technique attempts to equalize the means and variances of the quantization level histograms of each detector within a band by applying a gain and offset to the signals from each detector. Since this gain and offset is applied to a discrete function (histogram), and the result is still integer, the number of occupied quantization levels is not changed by the correction; only the total range they span is changed. This requires that some quantization levels within the expanded range be empty. The effect of this correction is illustrated in Figure 6. Although the histogram for an individual detector acquires some empty bins in the correction process (right-center), the histogram of the entire band is noticeably smoother (left-center). Of course, the cubic convolution resampling done in the geometric correction processing tends to equalize the histogram bin sizes even more (left-bottom).

The net effect of these corrections for a band with a fairly large variance, such as Band 4, illustrated here, is virtual elimination of any detector striping in the radiometrically corrected data. On the other hand, if a band has a lower variance, the histogram normalization is unable to equalize the means and variances of the detectors because of quantization limitations, and low level residual striping may exist after the correction. As an example, Figure 7 contains two plots for Band 2. The top plot is a trace of the mean signal level of each of the first 136 lines in a radiometrically and geometrically corrected image (CCT-PT). The lower plot was constructed by computing the mean signal level for each detector (on a CCT-AT) over the full frame and using these mean values to construct eight scans (128 lines) of data. Note the similarity of the two plots and the 17-line periodicity of the top trace compared with the

16-line period of the bottom. This 17- vs. 16-line period is due to the resampling to a slightly smaller pixel size in the geometrically corrected data. Note that this periodic fluctuation in mean signal level is not due to an error in the correction process; but stems from the round-off and/or truncation errors introduced when applying calibration transformations to discrete signals. The result is low level striping effects which will appear in the final image data even though the performance of the radiometric correction algorithm appears to be approaching its upper limits.

Low Frequency Noise

Analysis of low frequency noise (at or below scan mirror frequencies) produced the plots shown in Figures 8 and 9. In these figures, each trace is a plot of the mean signal level as a function of scan number for a given detector. The mean signal level for a detector for a scan is defined as the mean of all the pixels in that scan line. Figure 8 illustrates the consistent difference between forward and reverse scan signal levels for Band 6. As suggested by Figure 3b, the mean signal level for a forward scan is always lower than the mean signal for the following reverse scan, although the magnitude varies as one progresses down the frame.

Band 1, shown in Figure 9, contains several detectors which have significant low frequency variations. Detectors 4, 12, 10 and 8 have mean signal levels which vary between two states that are separated by approximately 2.0, 1.5, 1.0 and 0.75 signal counts, respectively. In other bands, this low frequency noise is much less evident, appearing in Band 2, Detector 1 (0.5 count), Band 3, Detectors 1 and 16 (0.5 count each), Band 5, Detector 10 (0.5 count) and Band 7, Detector 7 (0.5 count). Note that this low frequency variation may remain in the higher or lower state for several seconds, and is not to be confused with the high frequency, within-scan noise reported previously (as for Band 7, Detector 7) [5]. This low frequency effect could be serious in water-related applications where average signal levels are low.

Additional examination of the low frequency noise in Band 1 indicated that it was highly correlated between the noisy detectors (4, 12, 10 and 8). One would expect that within a given scan, the signal variations of each detector would be best correlated with the variations of the adjacent detectors, and least correlated with detectors spaced further in the array. Although this is strictly the case for Band 4, and generally true with the other bands, Band 1 is markedly different. The inter-detector correlation matrices for all seven bands are presented in Figures 10-16. As well as the above mentioned correlation of detectors 4, 12, 10 and 8 in Band 1, the tendency towards every-other detector correlation (odd/even detector effect) is quite noticeable in Bands 2, 3 and 7. The cause of this low frequency noise is under investigation; a preliminary hypothesis is that it is the result of the DC restore procedure locking onto the high (low) phase of the coherent noise reported elsewhere [6].

SUMMARY AND CONCLUSIONS

The overall quality of Thematic Mapper image data is very good. The spatial resolution is excellent and the radiometric correction procedures currently in use are working well, although some residual effects may remain which can cause low-level striping. Small but significant scan-direction effects exist in the reflective bands; they appear to be correctable in the two scenes examined by use of an empirical model employing exponential decay terms. Refinement and extension of the initial correction model await further understanding of the sensor phenomena driving the effect. Band 6 has a unique scan-direction effect, markedly different from the effect observed in the reflective bands. Highly correlated low frequency noise in Band 1, Detectors 4, 8, 10 and 12, may be due to a coherent-noise/DC-restore interaction; however, this phenomenon requires further investigation. It is recommended that any new radiometric correction procedures be integrated into a single process to minimize quantization and round-off effects.

The shorter wavelength of Band 1 and a scan-angle range larger than previous Landsats both increase the magnitude of scan-angle effect due to atmospheric and scene bidirectional reflectance characteristics in Thematic Mapper data. For a number of applications, approaches to reduce these effects should be developed.

References

1. W.A. Malila and R.F. Nalepka, "Atmospheric Effects in ERTS-1 Data, and Advanced Information Extraction Techniques," Proceedings of the Symposium on Significant Results Obtained from the Earth Resources Technology Satellite-1, NASA Goddard Space Flight Center, 1973, pp.1097-1104.

2. W.A. Malila, J.M. Gleason and R.C. Cicone, "Atmospheric Modeling Related to Thematic Mapper Scan Geometry", Final Report NAS9-14819, NASA Johnson Space Center, 1976.

3. J.V. Dave, "Extensive Data Sets of the Diffuse Radiation in Realistic Atmospheric Models with Aerosols and Common Absorbing Gases," Solar Energy, 21:361-369.

4. J. Engle, Private Conversation, 29 January 1983.

5. J.L. Barker, Presented at Landsat-D Investigations Workshop, NASA Goddard Space Flight Center, May 1982.

6. H.H. Kieffer, E. Eliason, P. Chavez, R. Batson and W. Borgeson, Presentation at Second Landsat-4 Investigations Workshop, NASA Goddard Space Flight Center, January 1983.

ORIGINAL PAGE IS
OF POOR QUALITY

FIGURE 1

SCAN-ANGLE EFFECT

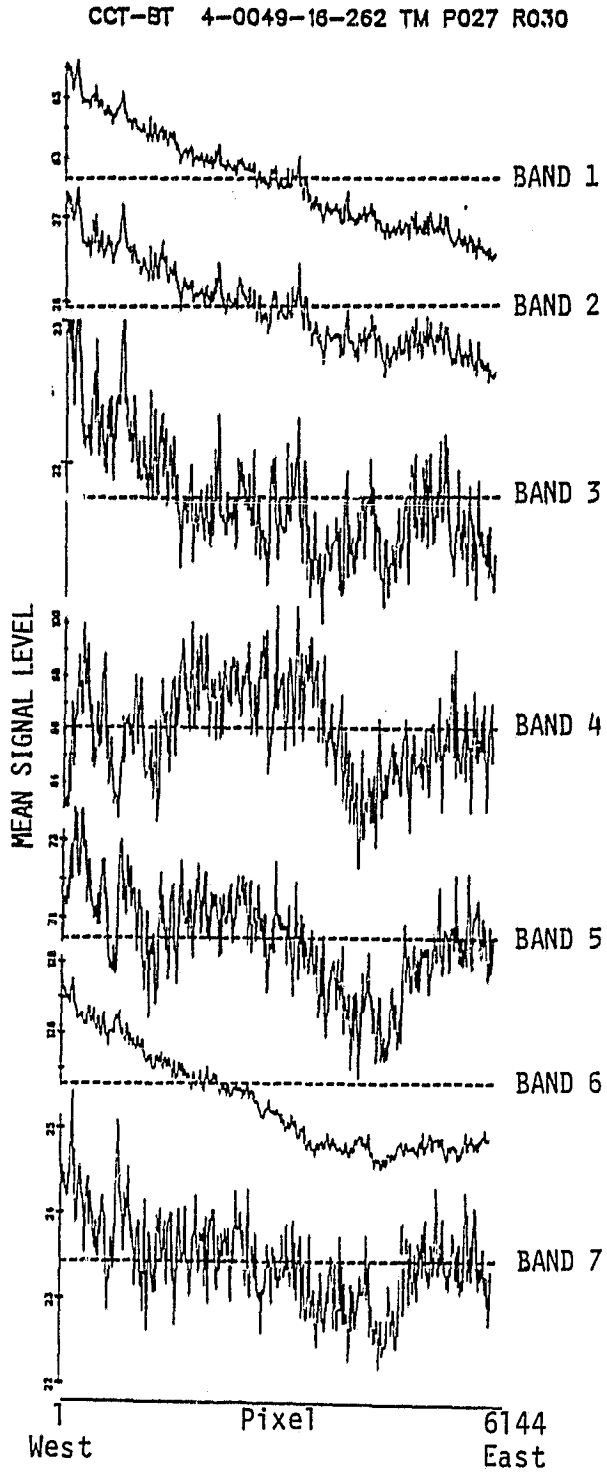

ERIM

FIGURE 2

ATMOSPHERIC SCAN-ANGLE EFFECTS IN MSS BANDS (MODEL RESULTS)

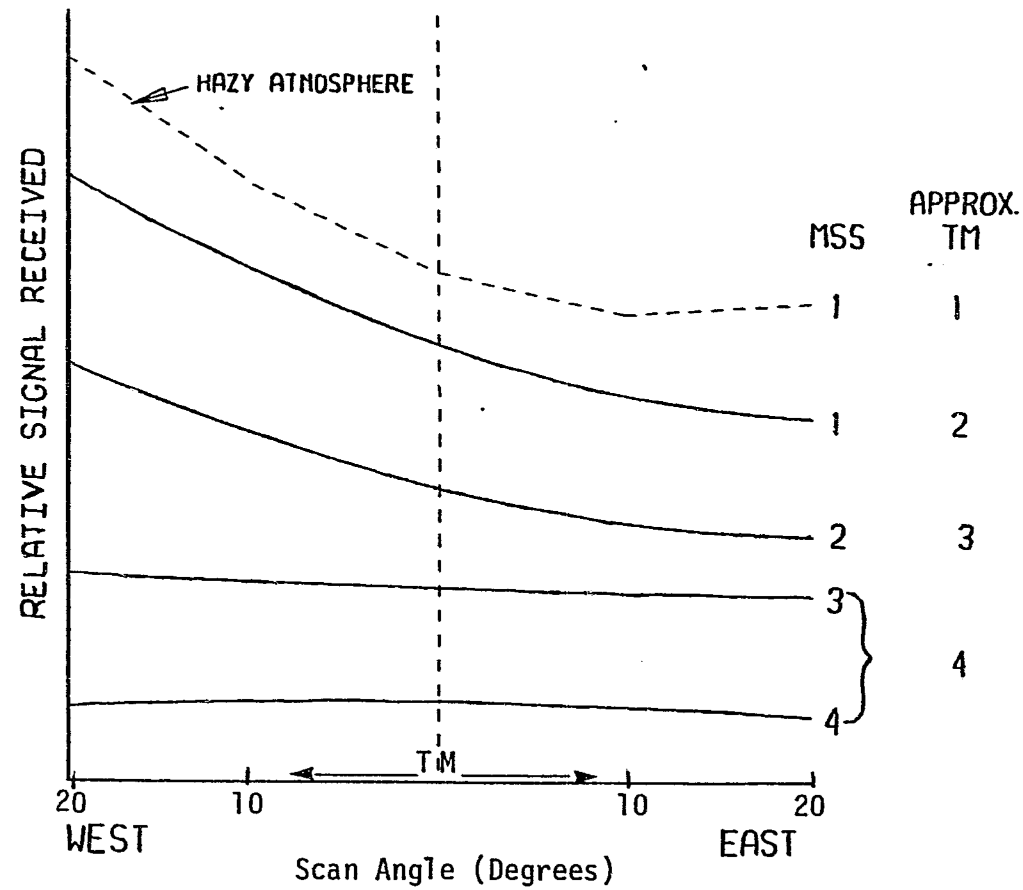

ERIM

FIGURE 3a

SCAN–DIRECTION EFFECT

CCT–BT 4–0049–16–262 TM P027 R030 BAND 1

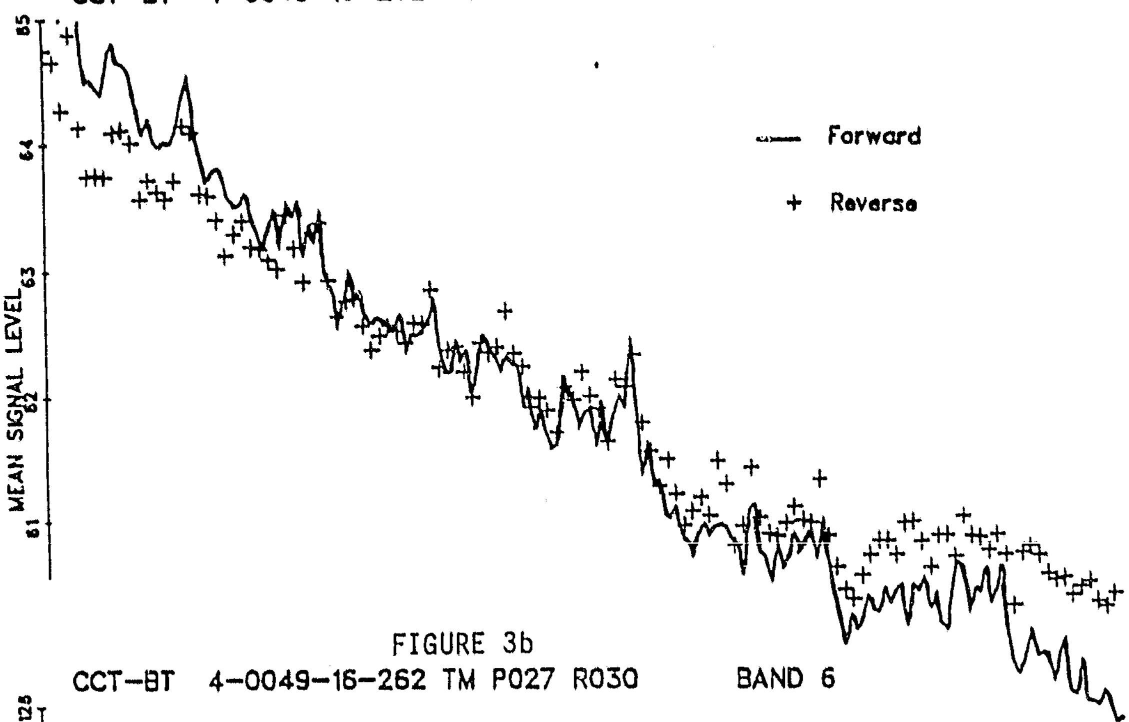

FIGURE 3b

CCT–BT 4–0049–16–262 TM P027 R030 BAND 6

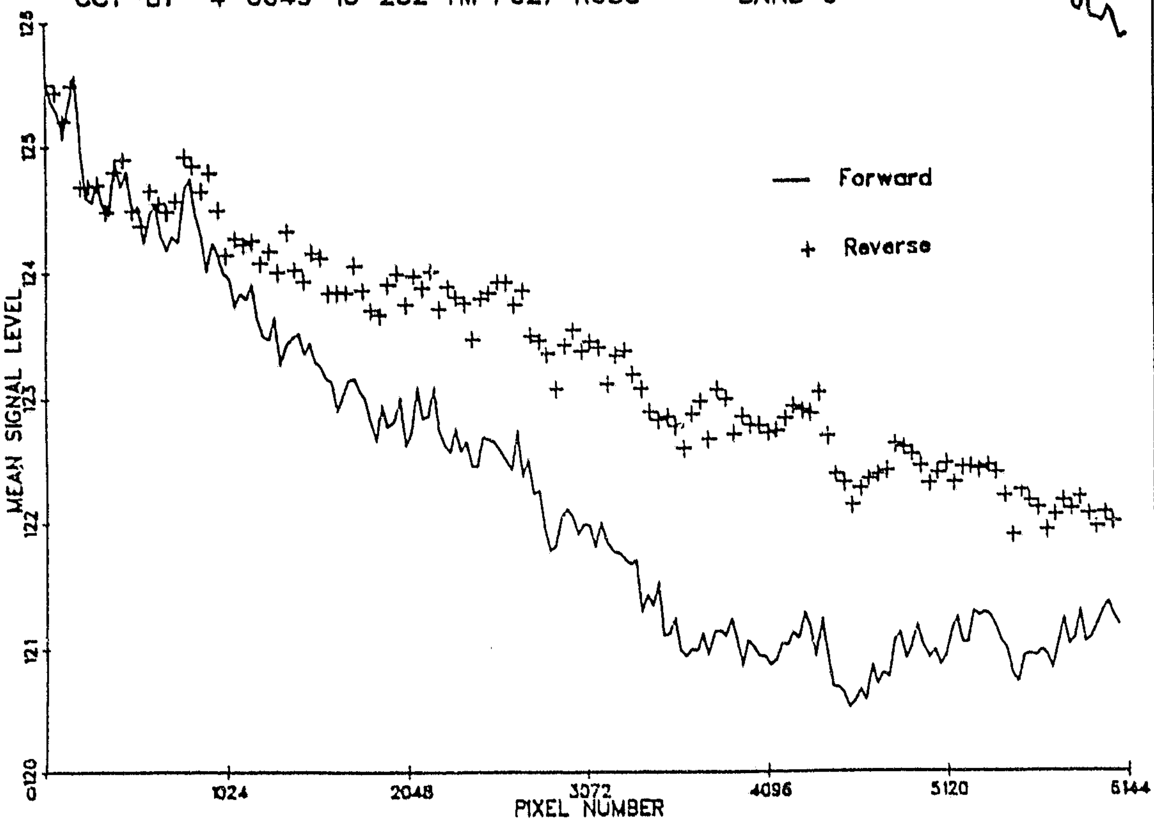

FIGURE 4

RATIO OF MEAN FORWARD TO MEAN MEAN REVERSE SCAN SIGNAL

Band 1

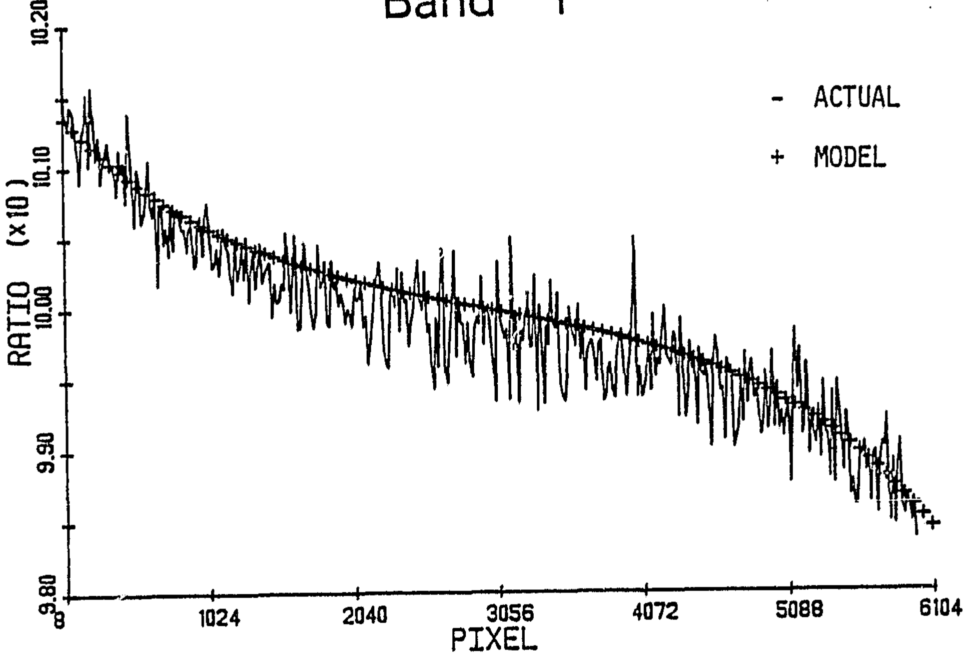

FIGURE 5

PREDICTED DECAY OF SIGNAL WITH TIME

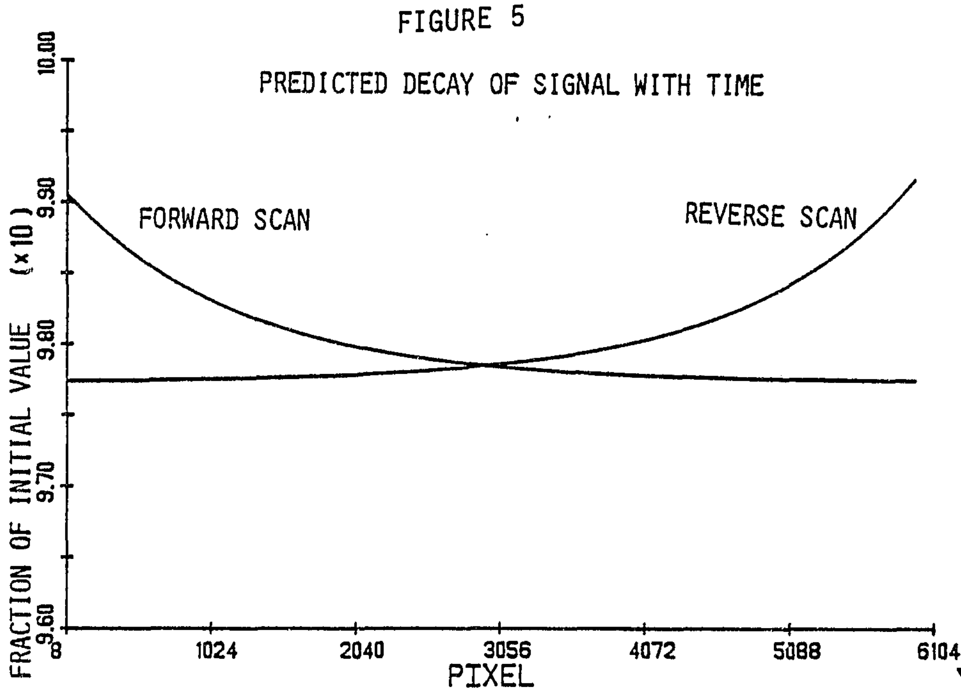

ERIM

FIGURE 6

QUANTIZATION-LEVEL HISTOGRAMS
THEMATIC MAPPER BAND 4

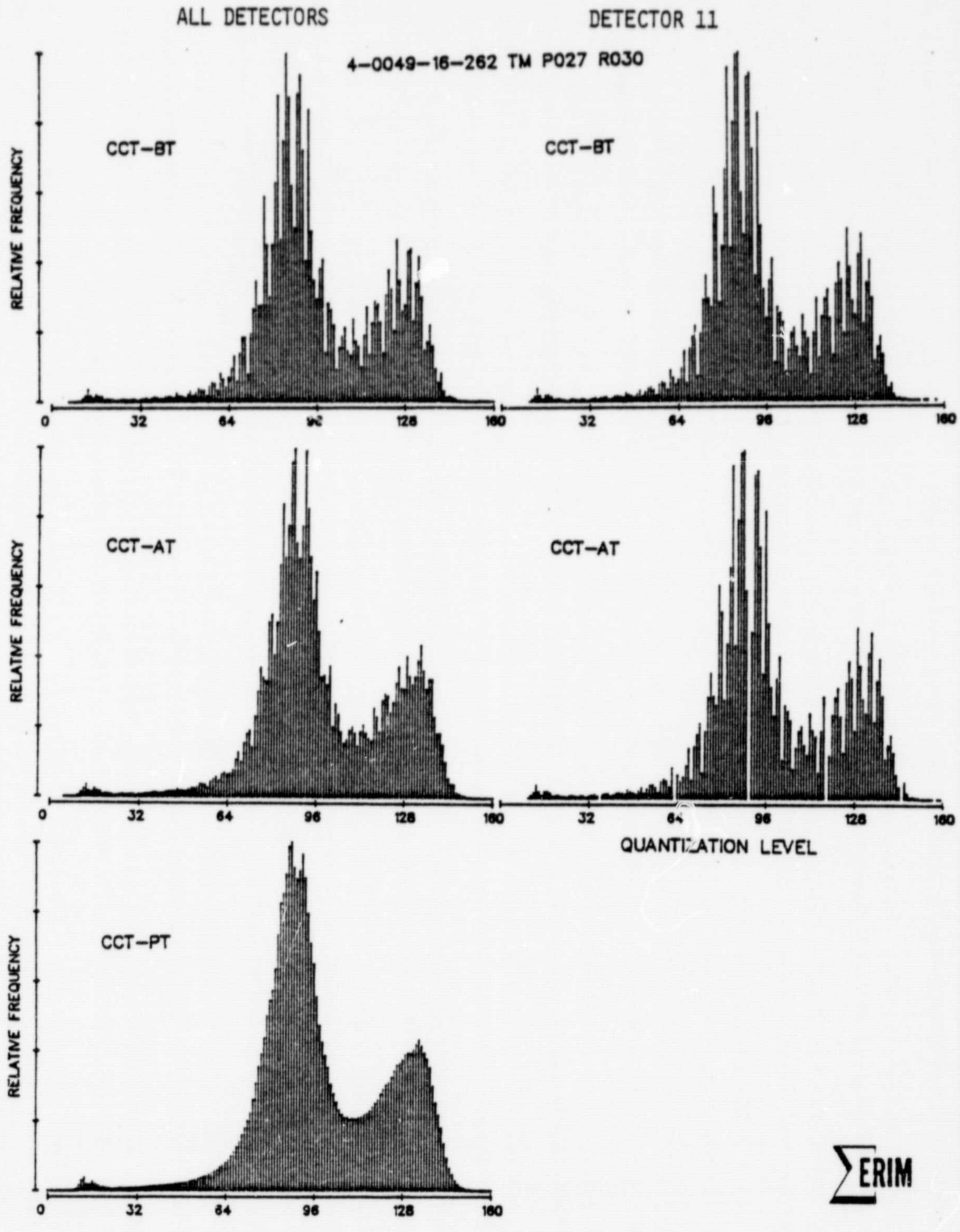

FIGURE 7

DOWN-TRACK MEAN SIGNAL

CCT-PT 4004916262 D02703082258 BAND 2

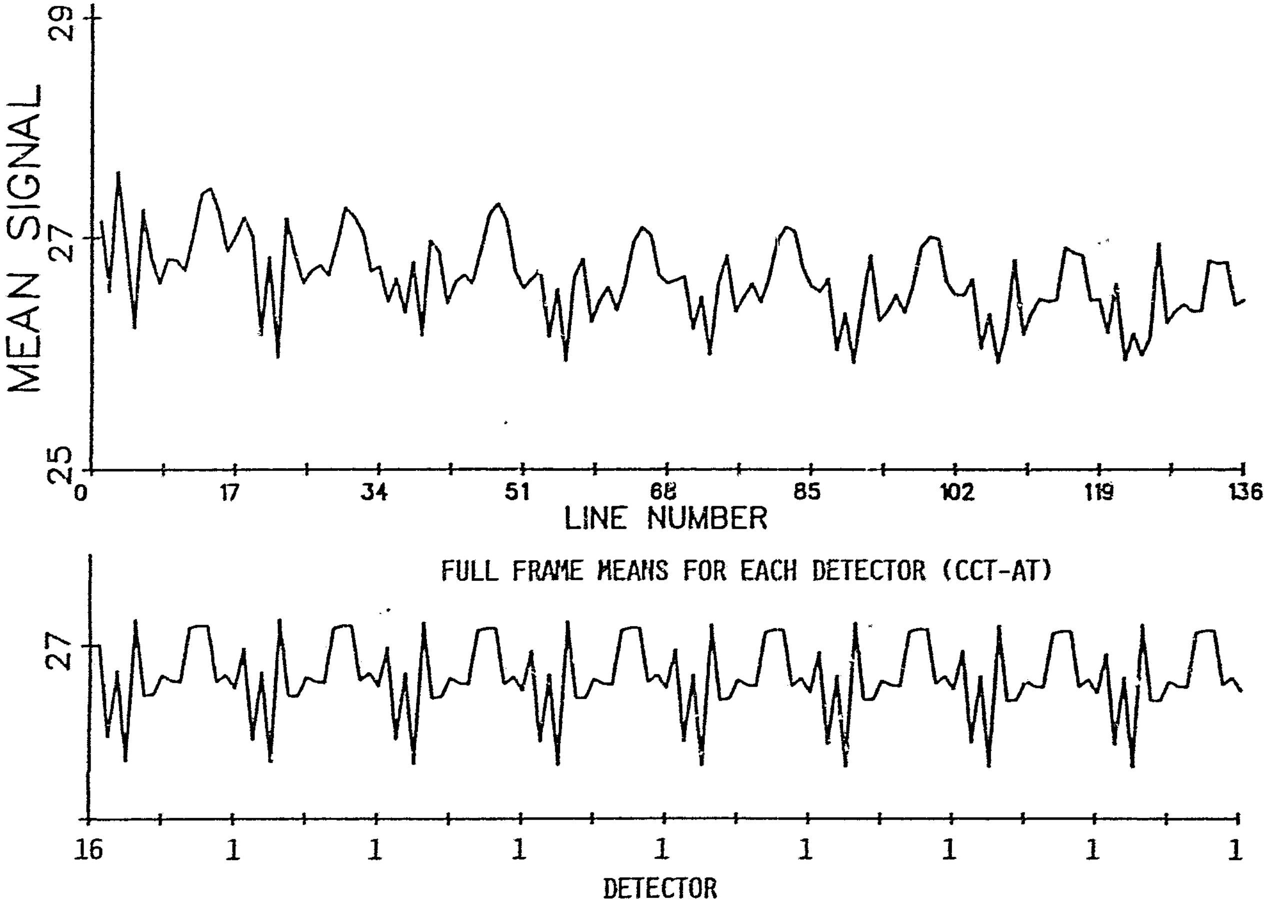

ERIM

ORIGINAL PAGE IS
OF POOR QUALITY

FIGURE 8

DOWN-TRACK TRACE OF SCAN-LINE MEAN SIGNAL FOR EACH DETECTOR IN BAND 6

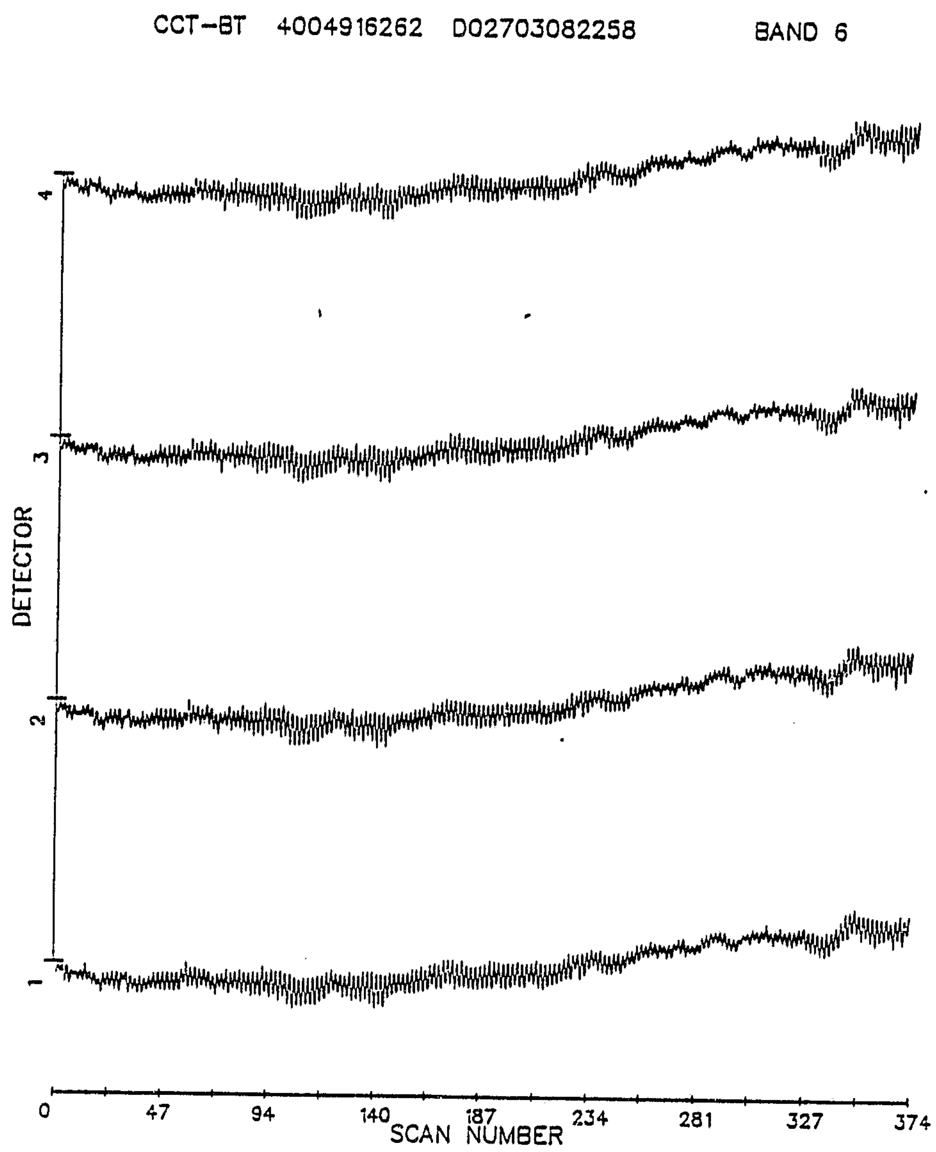

ERIM

FIGURE 9

DOWN–TRACK TRACE OF SCAN–LINE MEAN SIGNAL FOR EACH DETECTOR IN BAND 1

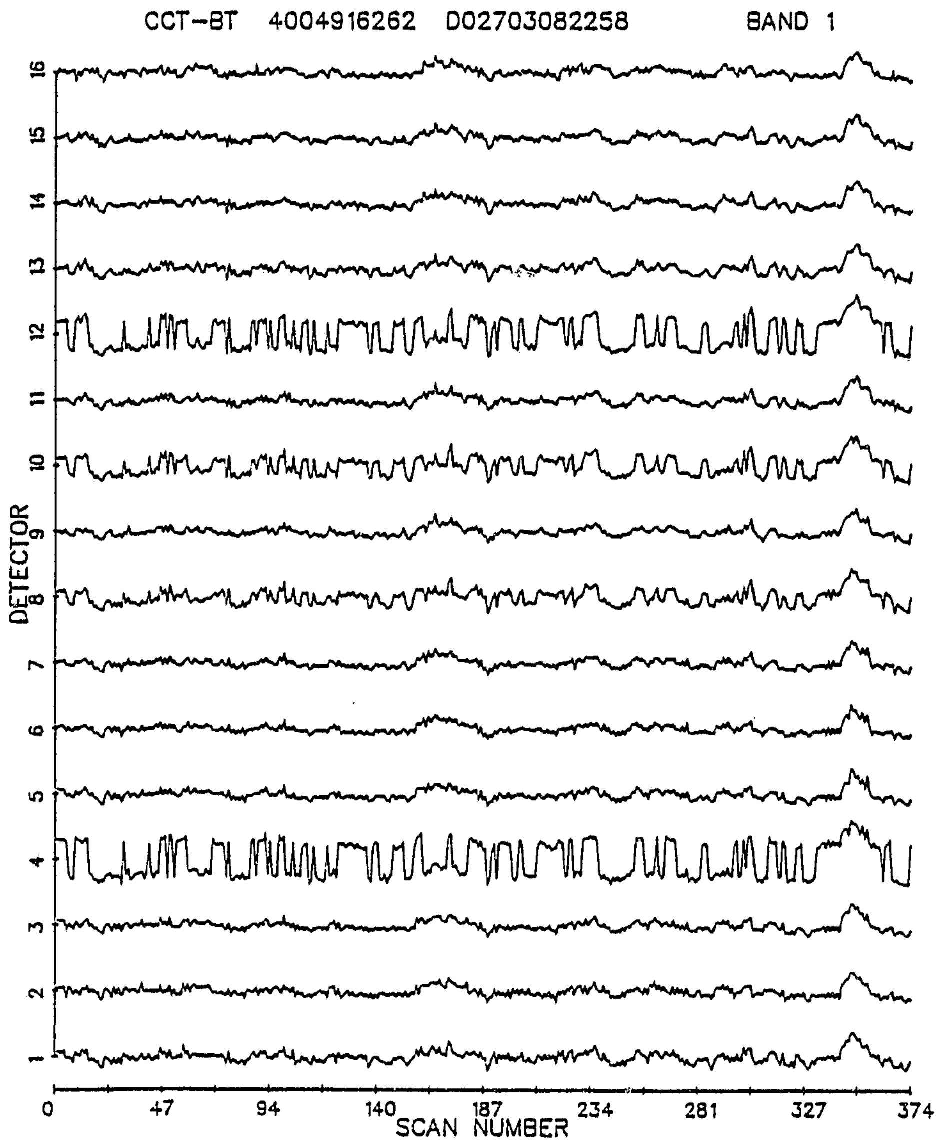

ERIM

ORIGINAL PAGE IS
OF POOR QUALITY

Correlation Matrix for Scan Line MEANS <1> BAND:1 CCT-BT 4004916262 (IOWA SCENE)

DET	1	2	3	4	5	6	7	8	9	10	11	12	13	14	15	16
1	1.00															
2	.82	1.00														
3	.90	.93	1.00													
4	.68	.19	.45	1.00												
5	.88	.87	.95	.48	1.00											
6	.80	.87	.92	.37	.95	1.00										
7	.84	.83	.91	.47	.94	.96	1.00									
8	.87	.55	.74	.87	.78	.71	.80	1.00								
9	.80	.74	.85	.50	.87	.90	.94	.80	1.00							
10	.81	.41	.63	.93	.68	.58	.68	.96	.72	1.00						
11	.85	.75	.86	.55	.88	.86	.91	.83	.94	.78	1.00					
12	.71	.23	.47	.98	.52	.40	.51	.90	.56	.96	.64	1.00				
13	.85	.64	.79	.70	.82	.77	.84	.89	.88	.87	.94	.78	1.00			
14	.82	.78	.84	.45	.86	.83	.86	.75	.85	.69	.92	.55	.92	1.00		
15	.82	.70	.82	.57	.83	.80	.85	.80	.88	.76	.93	.65	.95	.94	1.00	
16	.63	.81	.77	.09	.77	.78	.76	.47	.73	.36	.77	.19	.68	.87	.81	1.00

Note correlation of Detectors 4, 8, 10, 12 with each other lack correlations with others, especially Detectors 2 and 16.

FIGURE 10

CORRELATION BETWEEN DETECTORS OF LOW-FREQUENCY NOISE
TM BAND 1

Correlation Matrix for Scan Line MEANS <2> BAND:2 CCT-BT 4004916262 (IOWA SCENE)

DET	1	2	3	4	5	6	7	8	9	10	11	12	13	14	15	16
1	1.00															
2	.70	1.00														
3	.73	.67	1.00													
4	.72	.95	.63	1.00												
5	.83	.79	.91	.82	1.00											
6	.61	.90	.72	.91	.86	1.00										
7	.71	.74	.90	.74	.94	.88	1.00									
8	.62	.90	.67	.90	.82	.95	.86	1.00								
9	.78	.77	.84	.78	.92	.85	.94	.89	1.00							
10	.58	.87	.64	.87	.78	.92	.81	.96	.88	1.00						
11	.70	.70	.86	.69	.88	.80	.92	.82	.95	.85	1.00					
12	.55	.82	.67	.81	.77	.88	.81	.91	.86	.95	.89	1.00				
13	.84	.73	.77	.77	.88	.76	.84	.79	.92	.81	.91	.85	1.00			
14	.63	.85	.61	.86	.76	.86	.76	.89	.83	.92	.82	.94	.88	1.00		
15	.84	.71	.76	.74	.86	.73	.81	.76	.89	.78	.88	.81	.97	.86	1.00	
16	.40	.82	.44	.80	.59	[illegible]	.62	.85	.67	.88	.66	.88	.68	.91	.69	1.00

Note every other detector correlation, i.e., evens with evens, odds with odds.

FIGURE 11

CORRELATION BETWEEN DETECTORS OF LOW-FREQUENCY NOISE
TM BAND 2

Correlation Matrix for Scan Line MEANS <3> BAND:3 CCT-BT 4004916262 (IOWA SCENE)

DET	1	2	3	4	5	6	7	8	9	10	11	12	13	14	15	16
1	1.00															
2	.58	1.00														
3	.91	.72	1.00													
4	.61	.84	.85	1.00												
5	.89	.72	.96	.85	1.00											
6	.69	.88	.83	.90	.90	1.00										
7	.82	.67	.92	.84	.95	.89	1.00									
8	.55	.67	.77	.88	.78	.83	.89	1.00								
9	.60	.63	.78	.84	.79	.80	.89	.97	1.00							
10	.70	.82	.79	.79	.84	.91	.86	.82	.85	1.00						
11	.78	.57	.85	.75	.86	.76	.90	.84	.90	.88	1.00					
12	.52	.82	.66	.78	.71	.85	.74	.78	.79	.93	.80	1.00				
13	.84	.62	.85	.68	.87	.78	.87	.71	.77	.88	.93	.81	1.00			
14	.59	.82	.70	.75	.74	.35	.74	.73	.74	.92	.78	.95	.86	1.00		
15	.88	.51	.84	.59	.85	.68	.83	.62	.70	.78	.88	.66	.95	.75	1.00	
16	.17	.79	.29	.50	.36	.65	.32	.39	.36	.66	.30	.77	.41	.78	.29	1.00

Note preference for "every other" detector correlation as in Band 2.

FIGURE 12

CORRELATION BETWEEN DETECTORS OF LOW-FREQUENCY NOISE
TM BAND 3

Correlation Matrix for Scan Line MEANS <4> BAND:4 CCT-BT 4004916262 (IOWA SCENE)

DET	1	2	3	4	5	6	7	8	9	10	11	12	13	14	15	16
1	1.00															
2	.99	1.00														
3	.97	.99	1.00													
4	.96	.97	.99	1.00												
5	.94	.96	.97	.99	1.00											
6	.92	.94	.96	.97	.99	1.00										
7	.90	.92	.94	.96	.97	.99	1.00									
8	.89	.91	.92	.94	.96	.98	.99	1.00								
9	.87	.89	.91	.92	.94	.96	.98	.99	1.00							
10	.86	.87	.89	.90	.91	.94	.95	.97	.99	1.00						
11	.85	.86	.88	.89	.90	.92	.94	.96	.97	.99	1.00					
12	.83	.85	.86	.86	.88	.90	.92	.93	.95	.97	.99	1.00				
13	.83	.84	.85	.86	.87	.89	.90	.92	.94	.96	.97	.99	1.00			
14	.82	.84	.84	.85	.86	.88	.89	.91	.93	.94	.96	.97	.99	1.00		
15	.82	.83	.84	.84	.85	.87	.88	.89	.91	.93	.94	.95	.97	.99	1.00	
16	.81	.83	.83	.83	.84	.86	.87	.88	.89	.91	.92	.94	.95	.97	.99	1.00

Note correlation structure as expected, i.e., decreasing correlation with increasing inter-detector distance.

FIGURE 13

CORRELATION BETWEEN DETECTORS OF LOW-FREQUENCY NOISE
TM BAND 4

Correlation Matrix for Scan Line MEANS <5> BAND:5 CCT-BT 4004916262 (IOWA SCENE)

Dead Detector

DET	1	2	3	4	5	6	7	8	9	10	11	12	13	14	15	16
1	1.00															
2	.96	1.00														
3	.19	.05	1.00													
4	.89	.94	.05	1.00												
5	.85	.86	.32	.94	1.00											
6	.81	.86	.11	.94	.95	1.00										
7	.78	.81	.15	.88	.92	.97	1.00									
8	.73	.76	.21	.84	.88	.93	.96	1.00								
9	.71	.73	.23	.80	.86	.90	.94	.97	1.00							
10	.61	.64	.14	.71	.67	.76	.82	.78	.84	1.00						
11	.67	.69	.17	.75	.78	.82	.86	.90	.94	.85	1.00					
12	.64	.67	.03	.72	.72	.78	.82	.84	.88	.86	.97	1.00				
13	.64	.65	.17	.70	.73	.76	.79	.82	.87	.79	.95	.97	1.00			
14	.61	.63	.10	.68	.69	.73	.75	.78	.82	.76	.91	.95	.97	1.00		
15	.62	.60	.31	.63	.70	.69	.73	.76	.79	.67	.86	.87	.93	.95	1.00	
16	.60	.61	.10	.65	.65	.69	.70	.73	.74	.69	.82	.86	.89	.93	.95	1.00

FIGURE 14

CORRELATION BETWEEN DETECTORS OF LOW-FREQUENCY NOISE
TM BAND 5

Correlation Matrix for Scan Line MEANS <6> BAND:6 CCT-BT 4004916262 (IOWA SCENE)

DET	1	2	3	4
1	1.00			
2	.99	1.00		
3	.99	.99	1.00	
4	.99	.99	.99	1.00

FIGURE 15

CORRELATION BETWEEN DETECTORS OF LOW-FREQUENCY NOISE
TM BAND 6

Correlation Matrix for Scan Line MEANS <7> BAND:7 CCT-BT 4004916262 (IOWA SCENE)

DET	1	2	3	4	5	6	7	8	9	10	11	12	13	14	15	16
1	1.00															
2	.78	1.00														
3	.94	.78	1.00													
4	.73	.95	.79	1.00												
5	.89	.70	.95	.77	00											
6	.68	.89	.73	.95	.77	1.00										
7	.72	.25	.74	.31	.81	.35	1.00									
8	.56	83	.61	.88	.64	.94	.25	1.00								
9	.76	.67	.81	.72	.85	.78	.70	.81	1.00							
10	.48	.79	.51	.82	.53	.87	.13	.95	.75	1.00						
11	.74	.61	.77	.66	.82	.71	.70	.71	.93	.73	1.00					
12	.53	.73	.54	.77	.58	.81	.26	.86	.75	.92	.82	1.00				
13	.71	.58	.73	.62	.77	.65	.65	.66	.87	.68	.95	.82	1.00			
14	.61	.67	.61	.71	.65	.74	.41	.75	.75	.79	.85	.93	.90	1.00.		
15	.71	.55	.72	.59	.75	.61	.65	.60	.82	.60	.89	.74	.95	.88	1.00	
16	.55	.70	.55	.72	.57	.74	.27	.76	.67	.79	.74	.88	.79	.93	.84	1.00

Note "every other" detector correlation as in Bands 2 and 3, poor correlation of Detector 7 with others.

ORIGINAL PAGE IS OF POOR QUALITY

FIGURE 16

CORRELATION BETWEEN DETECTORS OF LOW-FREQUENCY NOISE
TM BAND 7